



Modelling Antarctic and Greenland volume changes during the 20th and 21st centuries forced by GCM time slice integrations

Philippe Huybrechts^{a,b,*}, Jonathan Gregory^{c,d}, Ives Janssens^b, Martin Wild^e

^aAlfred-Wegener-Institut für Polar- und Meeresforschung, Postfach 120161, D-27515 Bremerhaven, Germany

^bDepartement Geografie, Vrije Universiteit Brussel, Pleinlaan 2, B-1050 Brussels, Belgium

^cHadley Centre for Climate Prediction and Research, Meteorological Office, London Road, RG12 2SY Bracknell, UK

^dDepartment of Meteorology, University of Reading, Earley Gate, P.O. Box 243, RG6 6BB Reading, UK

^eInstitute for Atmospheric and Climate Science ETH, Swiss Federal Institute of Technology, Winterthurerstrasse 190, CH-8057 Zürich, Switzerland

Received 7 May 2003; received in revised form 19 September 2003; accepted 21 November 2003

Abstract

Current and future volume changes of the Greenland and Antarctic ice sheets depend on modern mass balance changes and on the ice-dynamic response to the environmental forcing on time scales as far back as the last glacial period. Here we focus on model predictions for the 20th and 21st centuries using 3-D thermomechanical ice sheet/ice shelf models driven by climate scenarios obtained from General Circulation Models. High-resolution anomaly patterns from the ECHAM4 and HadAM3H time slice integrations are scaled with time series from a variety of lower-resolution Atmosphere–Ocean General Circulation Models (AOGCM) to obtain the spread of results for the same emission scenario and the same set of ice-sheet model parameters. Particular attention is paid to the technique of pattern scaling and on how GCM based predictions differ from older ice-sheet model results based on more parameterised mass-balance treatments. As a general result, it is found that the effect of increased precipitation on Antarctica dominates over the effect of increased melting on Greenland for the entire range of predictions, so that both polar ice sheets combined would gain mass in the 21st century. The results are very similar for both time-slice patterns driven by the underlying time evolution series with most of the scatter in the results caused by the variability in the lower-resolution AOGCMs. Combining these results with the long-term background trend yields a 20th and 21st century sea-level trend from polar ice sheets that is however not significantly different from zero.

© 2004 Elsevier B.V. All rights reserved.

Keywords: Polar ice sheets; Climate change; Sea level rise; Greenhouse warming; Numerical modeling; Mass balance

1. Introduction

By far the largest amount of continental water is stored in the ice sheets of Antarctica and Greenland, which would add some 70 m to global sea level rise if they were to melt entirely. The average rate of mass exchange between these ice sheets and the oceans corresponds to about 6.5 mm/year of sea level change,

* Corresponding author. Alfred-Wegener-Institut für Polar- und Meeresforschung, Postfach 120161, D-27515 Bremerhaven, Germany. Tel.: +49-471-4831-1194; fax: +49-471-4831-1149.

E-mail address: phuybrechts@awi-bremerhaven.de (P. Huybrechts).

or 65 cm per century, implying that even relatively small imbalances between the average yearly snowfall and mass loss by surface melting and ice flow across grounding lines can have a significant effect, both for societies and the environment (Church et al., 2001). Despite considerable progress in observational data over the last decade, in particular from remote sensing platforms, the question of whether the polar ice sheets are in balance with the present-day climate can still not be answered with confidence (Rignot and Thomas, 2002), although large overall imbalances are increasingly considered unlikely. Large uncertainties are associated with future model predictions of ice sheet response, related to issues such as the evolution of greenhouse gas concentrations, the climate sensitivity to these changes, and the way such climate changes will affect the surface mass balance components of snow accumulation and meltwater runoff, which primarily determine volume changes on time scales less than a century (Huybrechts and de Wolde, 1999).

From a modeling point of view, it is convenient to distinguish between four components determining current and future volume changes of the polar ice sheets. The first component is the long-term background evolution as a result of ongoing ice-dynamic adjustment to past environmental changes as far back as the last glacial period. Superimposed on this long-term trend is the effect of modern mass-balance changes during the 20th and 21st centuries. Any deviation from their long-term average has an immediate effect on ice volume and thus on sea level. In addition, there is the ice-dynamic response to these modern surface mass-balance changes due to variations in the velocity field associated with changes in ice thickness and surface slope. As a fourth component one should also consider the possibility of ‘unexpected ice-dynamic responses’, which may or may not be related to contemporary climate changes, and which find their origin in variations at the ice sheet base or at the grounding line. Examples are the inferred thinning of the Pine Island and Thwaites sectors of the West Antarctic ice sheet (Shepherd et al., 2002) or the oscillatory behaviour of the Siple Coast ice streams (Joughin et al., 2002). Linked to this last category is the possibility of unstable behaviour, most importantly of a collapse of the West Antarctic ice sheet, but such behaviour is considered to be very

unlikely during the 21st century (Vaughan and Spouge, 2002; Bindshadler and Bentley, 2002). The distinction between the long-term trend and the response to 20th/21st century mass-balance changes is admittedly somewhat arbitrary, but is convenient to make from a modeling point of view because detailed forcing can only be generated for these centuries, whereas the long-term background forcing needs to be reconstructed from proxy data, and is therefore less detailed.

In this paper, we concentrate especially on the second and third components involving 20th and 21st century mass-balance changes and the ice-dynamic response these may entail. We use output from a suite of available General Circulation Models (GCMs) to prescribe climate changes over the ice sheets in an attempt to more realistically reproduce the spatial and temporal patterns of surface mass-balance changes. This approach bypasses many of the shortcomings evident in older work, which considered uniform or zonal averaged temperature changes and/or applied precipitation changes proportional to temperature changes (e.g. Huybrechts et al., 1991; De Wolde et al., 1997; Van de Wal and Oerlemans, 1997; Huybrechts and de Wolde, 1999). The latter studies were therefore unable to deal with the effects of changes in atmospheric circulation which could crucially impact on patterns of precipitation rate and temperature change, cf. Van der Veen (2002) for a critical assessment of sources of uncertainty in this older type of studies.

In recent years, several studies were performed that incorporated GCM output to force mass-balance changes. O’Farrell et al. (1997) forced an Antarctic ice sheet model with the transient accumulation field from a climate change simulation by the CSIRO Mk2 Atmosphere–Ocean General Circulation Model (AOGCM), and found equivalent sea-level lowerings of up to 50 cm after 500 years of integration. Van de Wal et al. (2001) linearly interpolated between two high-resolution GCM time slices from the ECHAM4 model (Wild and Ohmura, 2000) to obtain 70 years of Greenland ice sheet evolution. Their results highlighted the important role played by precipitation increases, which were found to largely compensate for increased runoff by the time of doubled CO₂ conditions. Huybrechts et al. (2002) and Fichfet et al. (2003) interactively coupled a Greenland ice sheet

model with an AOGCM to additionally investigate the effect of varying fresh-water fluxes on the oceanic circulation for the time period between 1970 and 2100. The latter work represents a further step to more fully investigate the interactions between the ice sheets, atmosphere, and ocean, but such simulations cannot be performed for long time periods and/or many climate scenarios because of the high computational cost involved.

The experiments discussed in this paper do not consider atmosphere or ocean feedback, but extend on work performed for the IPCC Third Assessment Report (Church et al., 2001). It uses the same ice sheet models and the same approach to derive the climate forcing, in which anomaly patterns from high-resolution time slice simulations are scaled with time series for a representative range of lower-resolution AOGCMs. The time-slice patterns have however been complemented with HadAM3H data from the Hadley Centre model to enable a comparison with the IPCC work that was based only on ECHAM4 output from the Max Planck Institute model. The ice sheet models have also been updated from Huybrechts and de Wolde (1999) as described in Huybrechts (2002) to incorporate new geometric datasets, a higher resolution of 20 km for Antarctica, updated accumulation datasets, and an improved melt and runoff model. The long-term background trend is analysed from the glacial cycle experiments in the latter study, which runs also serve as initial condition for the experiments discussed here. In order to better quantify the uncertainty introduced solely by the inter-model variability in climate response from current GCMs, all experiments were performed for the same emission scenario and the same set of ice-sheet and mass-balance model parameters. For Antarctica, the 20th/21st century simulations did not consider the effect of changes in basal melting below the ice shelves, as these have been investigated elsewhere and do not directly contribute to sea-level changes (Warner and Budd, 1998; Huybrechts and de Wolde, 1999).

2. The ice sheet model

The three-dimensional ice-dynamics models for Antarctica and Greenland are identical to those described in Huybrechts and de Wolde (1999) with all of

the updates as presented in Huybrechts (2002). The models consist of components describing the ice flow, the solid Earth response, and the mass-balance at the ice–atmosphere and ice–ocean interfaces. In the models, the flow is calculated in both the grounded ice, where it results from basal sliding and deformation, and, for Antarctica, in a coupled ice shelf to enable free migration of the grounding line. The flow is thermomechanically coupled by simultaneous solution of the heat equation with the velocity equations, using Glen's flow law and an Arrhenius-type dependence of the rate factor on temperature. Isostatic compensation of the bedrock takes into account the flexure of the rigid lithosphere and the viscous response of the underlying asthenosphere. Both models have a horizontal resolution of 20 km with 31 vertical layers in the ice, and another 9 layers in the bedrock for the calculation of the heat conduction in the crust. In the context of this paper, these ice-sheet models are used to determine the long-term background trend by simulating the Antarctic and Greenland ice sheets over the last few glacial cycles, and to determine the dynamic response to current and future mass balance changes.

The mass-balance model distinguishes between snow accumulation, rainfall, and meltwater runoff, which components are all parameterized in terms of temperature. The melt- and runoff model is based on the positive degree-day method and is identical to the recalibrated version as described in Janssens and Huybrechts (2000). It takes into account the process of meltwater retention by refreezing and capillary forces in the snowpack. This method to calculate the melt has been shown to be sufficiently accurate for most practical purposes, and seems more justified on physical grounds than often assumed (Ohmura, 2001). It moreover ensures that the calculations can take place on the detailed grids of the ice-sheet models so that one can properly incorporate the feedback of local elevation changes on the melt rate, features which cannot be represented well on the generally much coarser grid of a climate model. The melt model employed here has a somewhat larger sensitivity to temperature changes than older degree-day models, and its sensitivity also rises more quickly for positive perturbations. This is to a large extent due to the separate treatment of the rain fraction, which is generally found to contribute more to runoff than to

accumulation, and which fraction was often neglected in comparable mass-balance models previously. Inputs to the mass-balance model are the mean annual precipitation rate and the mean monthly surface temperature.

3. Climate forcing

To derive the climate forcing over the ice sheets we tried to make optimal use of currently available GCM simulations. Even for historical climate changes over the 20th century, an alternative is hardly available as there exist no direct observations of mass-balance changes over the ice sheets and there are only very limited records of basic climatic variables such as temperature and precipitation, most of them from the coast. The only other option would be to use meteorological re-analyses such as from ECMWF and NCEP-NCAR, but these only exist for the last 20 to 40 years and are known to have deficiencies over the ice sheets because of little observational constraint and questionable parameterizations, probably more so for Antarctica than for Greenland (Bromwich et al., 1998; Hanna and Valdes, 2001).

Direct coupling between GCMs and ice-sheet models would be desirable but is not yet feasible because of the wide gap between typical GCM resolutions in the range of 100–500 km and the much finer grids required for ice-sheet models to properly deal with the width of ablation zones and the channeling of the flow at the margin.

In our analysis, we make a distinction between the patterns of climate change on the one hand, and the transient climate evolution over time on the other. The former are derived from GCM simulations at the highest horizontal resolution currently used in climate modeling, but such simulations can only be performed for short periods of time. We therefore adopt a method to scale these anomaly patterns with ice-sheet averaged variables obtained from transient AOGCMs at lower resolution in order to produce continuous forcing under conditions of climate change.

3.1. Climate anomaly patterns

The climate anomaly patterns are derived from so-called time-slice experiments (Cubasch et al., 1995).

Thereby a high-resolution atmospheric model is run for a limited time window, using prescribed boundary conditions of sea surface temperature (SST) and sea-ice distribution, which are derived from a lower-resolution, transient coupled atmosphere–ocean scenario run. Model resolutions of typically 50–100 km in polar regions allow for a more realistic topography crucial to better resolving temperature gradients and orographic forcing of precipitation along the steep margins of the polar ice sheets.

We used time-slice output from a present-day and a 21st-century climatic change experiment from two available models. Both model experiments were set up in a similar way. The present-day experiments use observationally constrained SST as boundary condition, to which anomalies from the lower-resolution driving AOGCM are added to produce boundary conditions for the high-resolution model during the anomaly period.

The first model is the ECHAM4 GCM developed at the Max Planck Institute in Hamburg (Roeckner et al., 1996). This model is implemented on a spectral T106 ($\sim 1.125^\circ \times 1.125^\circ$) resolution. The transient scenario run was performed with ECHAM4 at T42 ($\sim 2.8^\circ$) resolution coupled to the OPYC3 ocean model (Roeckner et al., 1999). This coupled experiment takes into account a gradual increase in CO₂ and other greenhouse gas concentrations according to the IPCC scenario IS92a (Leggett et al., 1992). The two time slice experiments were run for 10 years each for the decades 1971–1980 and 2041–2050, at which time the CO₂ concentration is expected to double. The present-day experiment used the Atmospheric Model Intercomparison Project (AMIP) SST climatology, superimposed with detrended SST variabilities from the lower-resolution AOGCM transient run. The 21st-century climatic change time-slice experiment used the SST obtained through a superposition of the AMIP SST climatology with the mean SST changes between the present-day period and the 21st century climate change period and the SST variabilities for the 21st century climate change period, both taken from the coupled lower resolution transient experiment. In this paper we use the differences of the time slices averaged over both decades, taken to be centred over the years 1975 and 2045, respectively. The resulting anomaly patterns of precipitation and temperature over Greenland and Antarctica were discussed in

more detail in Wild and Ohmura (2000) and Wild et al. (2003).

The second model is the HadAM3H GCM developed at the Hadley Centre for Climate Prediction and Research. The high resolution time slice run is performed with the atmospheric component only at $1.875^\circ \times 1.25^\circ$ resolution. This is done for the periods 1960–1990 and 2070–2100, respectively, hence the present-day patterns are also conveniently centred at the year 1975, though the period separating the two time slices is 40 years longer compared to the ECHAM4 time slices (2085 against 2045). The 30-year time-slice window also ensures statistically more significant results than was possible for the 10-year period of the ECHAM4 results for reasons of shortage of CPU time. The driving AOGCM is HadCM3 at $2.5^\circ \times 3.75^\circ$ horizontal resolution (Pope et al., 2000; Gordon et al., 2000). In this experiment, the SRES A2 scenario was used (Nakicenovic et al., 2000), similar to the older IS92a scenario used for the ECHAM4 results. Both the control and anomaly runs are the means over an ensemble of three independent runs, which further reduces statistical noise. The HadAM3H 2071–2100 SST fields were constructed by adding HadCM3 SST anomalies to HadISST (observed SSTs) for 1961–1990. This was done in such a way as to preserve the HadCM3 trend through the period 2071–2100, but retain the interannual variability of HadISST. The HadAM3H sea ice concentrations were derived in the same way from HadISST sea ice. Large local changes are associated with the retreat of sea ice.

Because the HadCM3 control sea ice distribution is not entirely realistic, features associated with climate change might be misplaced with respect to the position of the sea ice edge in HadISST. Therefore a final adjustment was made to map the HadCM3 SST and sea ice changes to the HadISST sea ice concentration field.

Figs. 1 and 2 demonstrate to what extent the high-resolution time-slice simulations are able to reproduce the current precipitation distribution. The simulated fields are not entirely compatible with the observations as the GCM fields are for total precipitation and the observations are for precipitation minus evaporation or sublimation. Since the observed fields over the ice sheets are in fact derived from accumulation measurements, they also contain an unknown contribution from deflation, so that the simulated precipitation should at least be equal or higher than the observed fields. Nevertheless, despite these reservations the comparison shows that the AGCMs are very capable of reproducing the broad patterns of the precipitation distribution. That is mainly because the topography can be reasonably resolved on a $1\text{--}2^\circ$ grid. For both ice sheets and both GCMs there is however a tendency to slightly underestimate precipitation over the dry plateau areas and somewhat overestimate precipitation at the margin. The simulated precipitation totals are all between 4% and 25% higher than the total ice-sheet accumulation/precipitation as reconstructed from in-situ measurements (Table 1), which seems very reasonable as the simulated fields do not incorporate

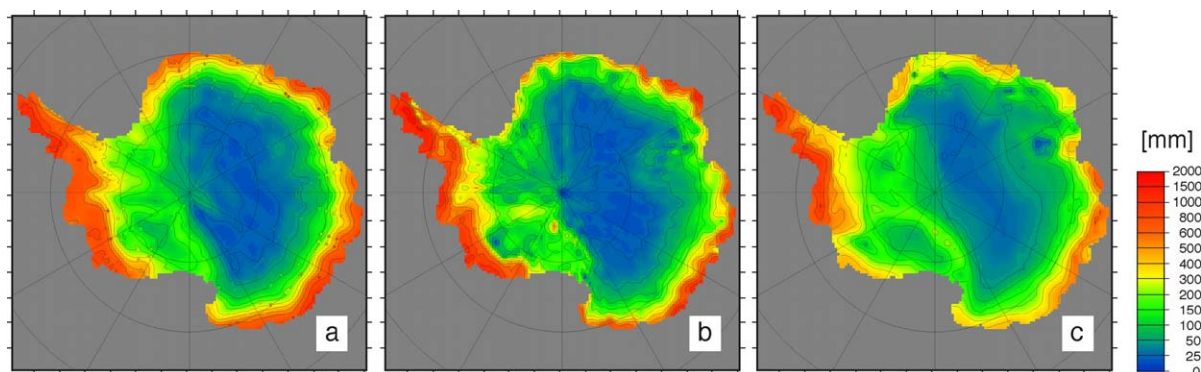


Fig. 1. High-resolution time slice simulations of the present-day total precipitation rate over Antarctica. (a) ECHAM4. (b) HadAM3H. For comparison, panel c shows the accumulation rate over the ice sheet in the same units (mm/year of water equivalent) for the distribution, which is used as input in the ice-sheet model. The latter is a modification of the Giovinetto data set as presented in Huybrechts et al. (2000).

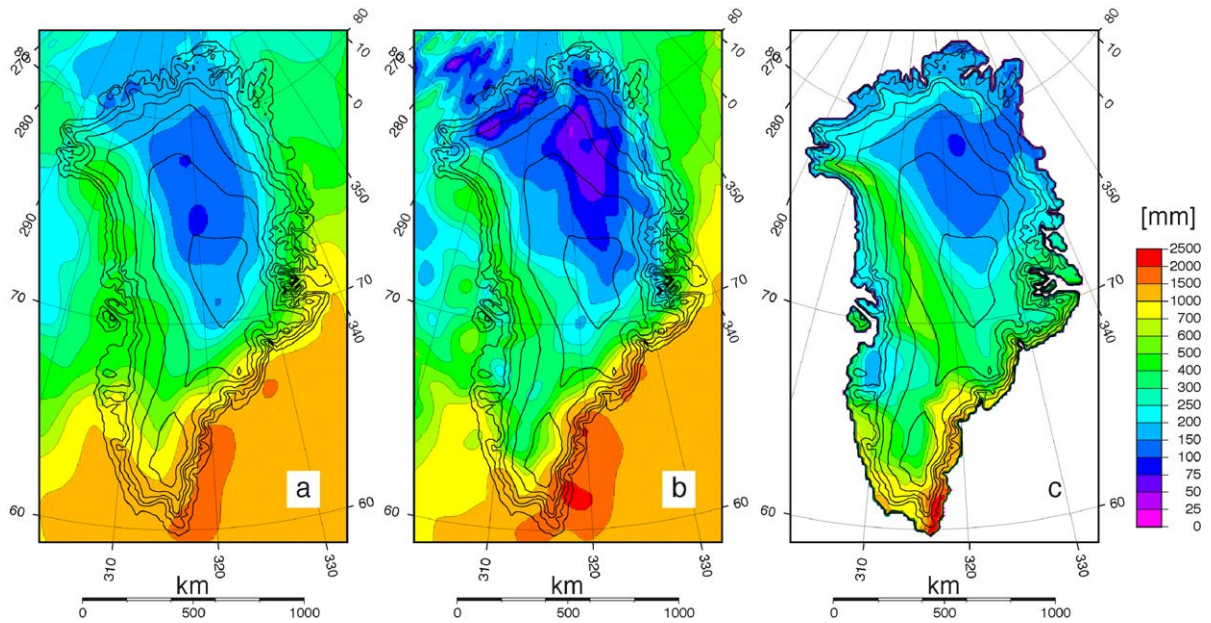


Fig. 2. High-resolution time slice simulations of the present-day total precipitation rate over Greenland. (a) ECHAM4. (b) HadAM3H. For comparison, panel c shows the mean annual precipitation rate for the distribution that is used as input in the Greenland mass-balance model. The latter is a modification of the Ohmura and Reeh (1991) distribution to include shallow ice-core data from AWI traverses in northern Greenland during the 1990s (Jung-Rothenhäusler, 1998). All values are expressed in mm/year of water equivalent.

sublimation and wind-blown snow, and therefore are expected to have higher values. The comparison certainly enhances confidence in the quality of the time-slice experiments, though it is noted that the mass-balance calculations in this paper are performed

in anomaly mode and therefore do not make direct use of these simulated precipitation fields.

The actual anomaly patterns as they are used in the mass-balance calculations are displayed in Figs. 3 and 4. A number of basic statistics of these fields are listed

Table 1

Rates of ice-sheet averaged precipitation and temperature changes from the AGCM time slices and their underlying driving time series

	Greenland ECHAM4	Greenland HadAM3	Antarctica ECHAM4	Antarctica HadAM3
Mean annual temperature difference AGCM time slice [$^{\circ}\text{C}/\text{century}$]	+4.83	+4.09	+2.53	+3.35
Mean annual temperature difference driving AOGCM time series [$^{\circ}\text{C}/\text{century}$]	+4.71	+4.58	+3.42	+3.48
Mean summer temperature difference AGCM time slice [$^{\circ}\text{C}/\text{century}$]	+3.94	+3.44	+2.83	+3.34
Mean annual precipitation anomaly AGCM time slice [%/century]	+42.4	+20.7	+19.5	+19.6
Mean annual precipitation anomaly driving AOGCM time series [%/century]	+49.8	+27.5	+20.2	+15.0
Mean precipitation sensitivity AGCM time slice [%/ $^{\circ}\text{C}$]	+7.60	+4.71	+7.31	+5.46
Mean precipitation sensitivity driving AOGCM time series [%/ $^{\circ}\text{C}$]	+8.96	+5.44	+5.53	+4.09
Effective sea-level sensitivity (precipitation only) [mm/year/ $^{\circ}\text{C}$]	-0.133	-0.090	-0.492	-0.369
Average ice-sheet model input precipitation/accumulation rate [m/year ice equivalent]	0.356	0.356	0.186	0.186
Ratio of AGCM time slice precipitation to ice-sheet model input precipitation/accumulation	1.154	1.039	1.242	1.102

Values are over grounded ice only, and normalized to a century, taking into account that the ECHAM4 results were for a duration of 70 years (1975–2045) and the HadAM3H results for a period of 110 years (1975–2085). Mean summer temperature is the average for the months JJA (Greenland) or DJF (Antarctica). The effective sea-level sensitivities are for precipitation changes only and calculated by superimposing the time-slice anomalies on the input precipitation/accumulation distributions used in the ice-sheet mass-balance model.

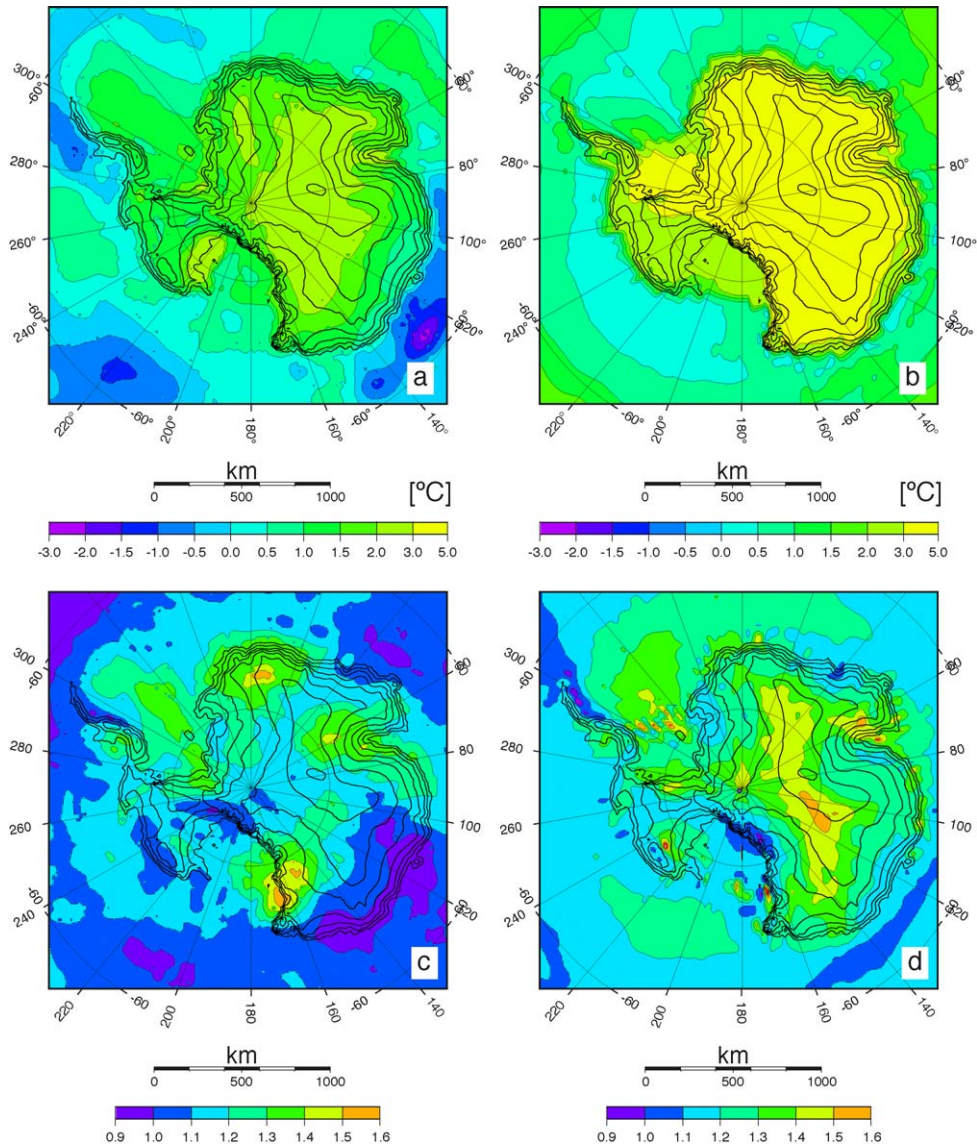


Fig. 3. Climatic anomaly patterns over Antarctica from the high-resolution time-slice experiments used to calculate changes of the mass-balance. The upper panels (a,b) show mean summer (DJF) surface air temperature differences at the 2 m level. The lower panels (c,d) are for mean annual precipitation ratios. The left panels (a,c) are from the ECHAM4 model; the right panels (b,d) are from the HadAM3H model. Note that while the legends for both climate models are the same, the climate anomalies refer to different time periods.

in Table 1. When comparing the anomaly patterns between the ECHAM4 and HadAM3H models, one should take into account that the former correspond to a time difference of 70 years and the latter to 110 years. Also, the underlying emission scenario of the driving AOGCM is slightly different. Nevertheless, there are some striking similarities between the two GCMs,

especially concerning temperature changes. Both models display a more or less concentric pattern of summer warming which becomes stronger with elevation. The average summer warming is lower than the annual mean for Greenland, but not for Antarctica, and mean annual warming rates over the respective simulation periods are of comparable magnitude.

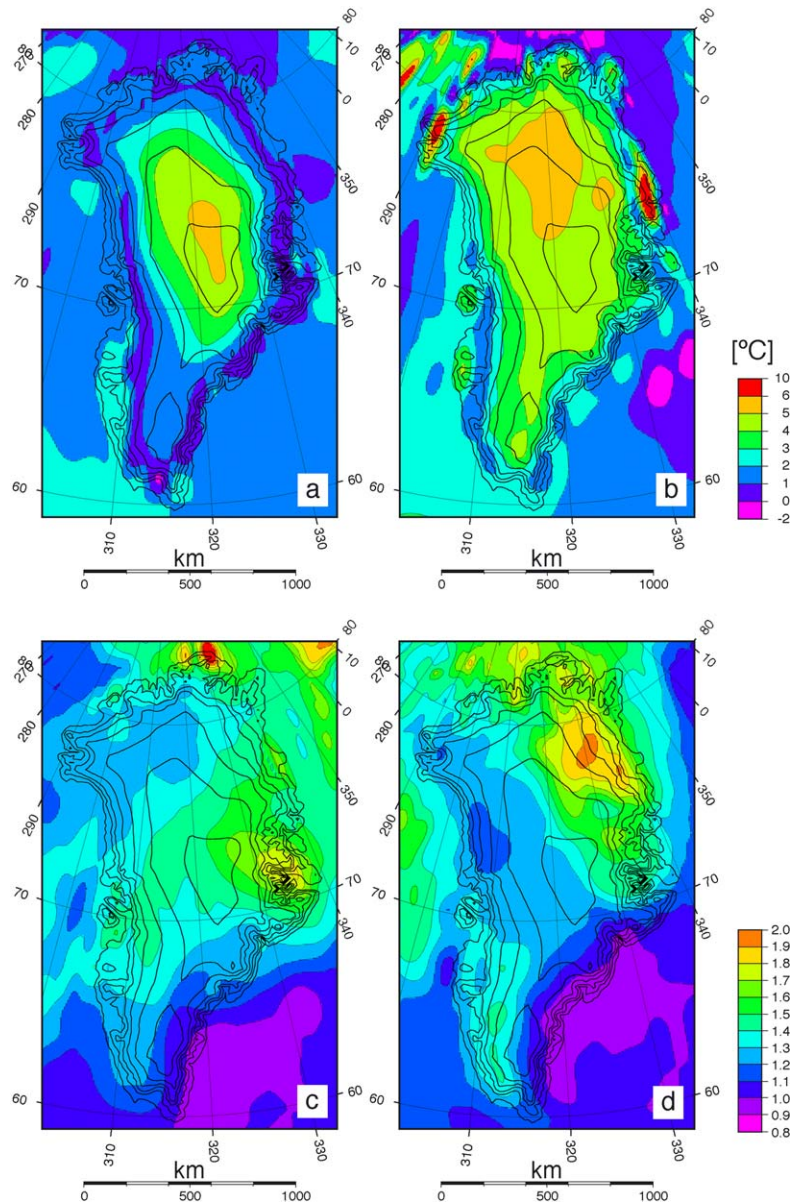


Fig. 4. Climatic anomaly patterns over Greenland from the high-resolution time-slice experiments used to calculate changes of the mass-balance. The upper panels (a,b) show mean summer (JJA) surface air temperature differences at the 2 m level. The lower panels (c,d) are for mean annual precipitation ratios. The left panels (a,c) are from the ECHAM4 model; the right panels (b,d) are from the HadAM3H model. Note that while the legends for both climate models are the same, the climate anomalies refer to different time periods.

The crucial parameter for melting is summer temperatures around the ice-sheet margin, where the ablation takes place. For Antarctica, both GCMs simulate coastal warmings below 2 °C for the 21st century. As present-day summer temperatures are

presently too low to cause any significant runoff (e.g. Table 11.6 in Church et al., 2001), it can be expected that surface melting will continue to be of little importance, even under greenhouse warming conditions during the 21st century. Over Greenland,

both AGCMs likewise simulate comparatively little summer warming over the ablation zone, which is equally found to be in the range of 0–3 °C, with the lower values for the ECHAM4 experiment. The smaller increase in the summer temperature around the margin may be due to dampening from the nearby ocean, which hardly warms in both experiments, or dampening over a melting ice surface as its temperature is limited to the melting point and therefore cannot rise further. A thorough meteorological explanation of this feature has however not yet been given.

Concerning precipitation changes under enhanced greenhouse warming conditions, both time-slice experiments agree that the ice-sheet averaged values should increase by amounts of between 20% and 40% per century (Table 1). These increases are related to slight poleward displacements of polar lows and the higher moisture-holding capacity of the warmer air. There is some qualitative agreement that the relative precipitation increase is stronger over higher elevations, but in general both AGCM patterns show relatively little resemblance, though the normalized average rate of Antarctic precipitation increase is for both time-slice experiments almost the same at a little less than 20% per century. The maximum predicted local precipitation increase is at most a doubling by the end of the 21st century as occurring in northeast Greenland in the HadAM3H model. On average, the predicted precip-

itation increase is also larger for Greenland than for Antarctica.

3.2. Climatic time series

The transient time series for scaling the high-resolution anomaly patterns were all derived from AOGCM simulations which considered historical greenhouse gas concentrations during the 20th century, and used the IS92a scenario for the 21st century including the tropospheric sulphur cycle. These experiments are the same set of model simulations used for the IPCC TAR (Houghton et al., 2001) and enable to determine the inter-model variability for the same greenhouse warming scenario (Table 2). Atmospheric resolutions in these simulations are typically 3–5° in latitude/longitude and 1–5° for the oceanic component, cf. Tables 8.1 and 9.1 of the IPCC TAR. These runs are somewhat different from the driving AOGCMs of the time-slice simulations, which are further referred to as ECHAM4/OPYC3 G and HadCM3 A2. This is however not crucial for the work discussed in this paper, as the scaling technique is independent from the emission scenario that was originally used to obtain the time slice results.

Fig. 5 displays the ratio of ice-sheet averaged mean annual precipitation and the difference of ice-sheet averaged mean annual temperature over Greenland and Antarctica from all these time series. Apparently,

Table 2
An overview of the coupled AOGCM runs used to scale the time slice patterns

AOGCM model name	Length of simulation period [years]	Equilibrium climate sensitivity [°C]	Polar amplification over Antarctica	Polar amplification over Greenland
CGCM1 GS	1900–2099	3.5	1.1	1.3
CSIRO Mk2 GS	1880–2100	4.3	1.1	2.0
CSM 1.3 GS	1870–2099	2.2	1.1	3.1
ECHAM4/OPYC3 GS	1860–2049	2.6	1.5	1.2
GFDL_R15_a GS	1766–2065	3.7	0.8	1.9
HadCM2 GS	1860–2099	4.1	1.2	1.4
HadCM3 GSIO	1860–2098	3.3	1.3	1.4
MRI2 GS	1900–2100	2.0	1.2	1.6
DOE PCM GS	1870–2099	2.1	1.6	2.2

These experiments consider historical greenhouse gas concentrations until 1990, followed by a scenario equivalent to IS92a for the 21st century, taking into account the effect of sulphate aerosols. The equilibrium climate sensitivity is defined as the change in global mean temperature resulting from a doubling of the atmospheric CO₂ concentration after the model attains a new equilibrium. The polar amplification expresses the ratio between the average surface air temperature change over the respective ice sheets and the global mean. A comprehensive list of other model details and references is provided in Tables 8.1 and 9.1 of the IPCC TAR (Houghton et al., 2001).

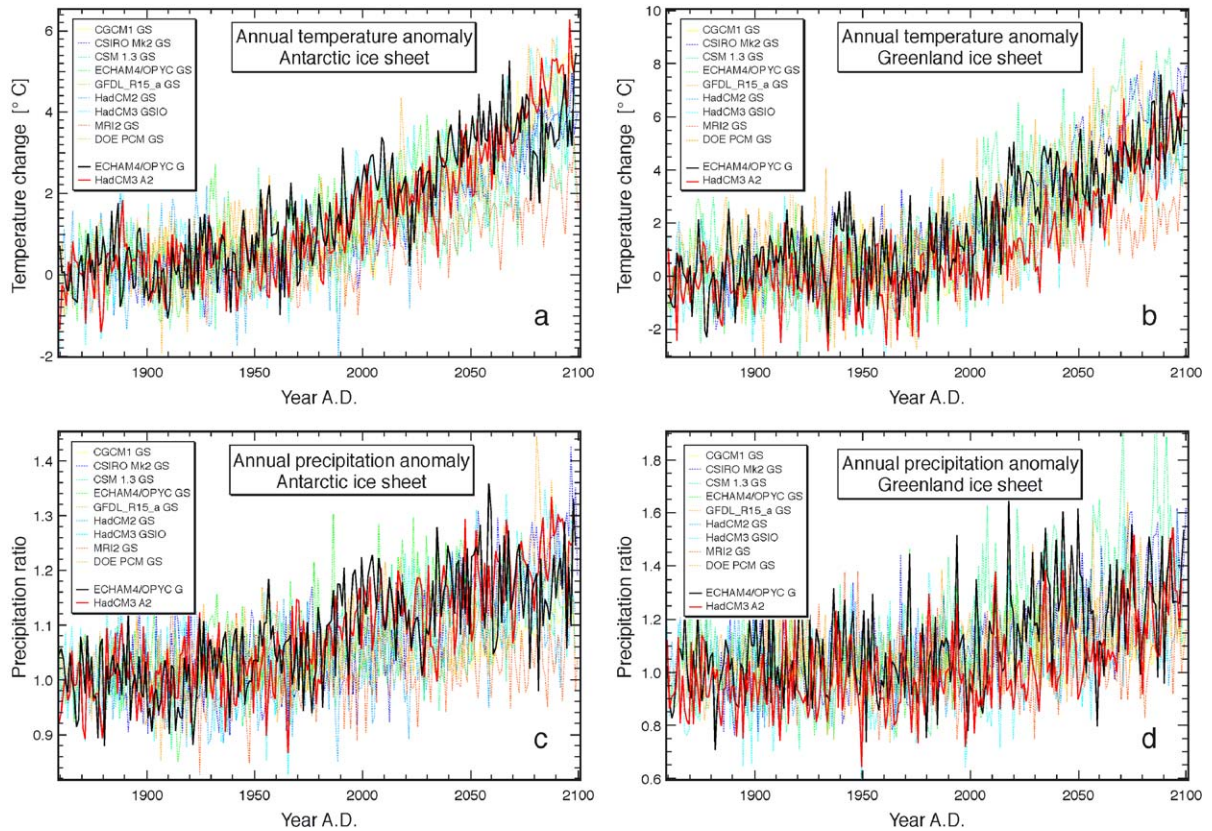


Fig. 5. Climatic time series for the 20th and 21st centuries from the lower-resolution AOGCM simulations used to force the higher-resolution time slice patterns. Values are mean annual averages over the respective ice sheets. These all followed the IS92a scenario. The red and black lines are for the low-resolution AOGCM simulations used for driving both the high-resolution time-slice experiments.

there is quite a lot of variability. Whereas it is hard to distinguish a clear trend for the 20th century, all curves have in common that there is a clear rise for the 21st century. Typical warmings by the end of the 21st century are of the order of 3 °C for Antarctica and 4 °C for Greenland, higher than the global average by a factor 1 to 3 because of the polar amplification (Table 2). The concomitant increases in precipitation are between 10% and 50% for both ice sheets.

3.3. Pattern scaling technique

To eliminate systematic errors and minimize the effects of the still rather coarse resolution of the climate models as compared to the ice-sheet model, all climatic changes are considered in the perturbation (anomaly) mode. That is necessary because the

absolute GCM climate data differ from the observations and because the ice-sheet margin, where the run-off takes place, is generally narrower than the model resolution, even at the resolution of the time-slice simulations. The approach additionally ensures that the present-day fields of precipitation rate and surface temperature can be represented in the best possible way from observations. Since ice-sheet melting is determined locally on the ice-sheet model grid, the calculation can also properly deal with the temperature effect of elevation changes in addition to those from climate changes. For the time series, climatic perturbations are considered at the same instant of time for the climate change run and the control run to eliminate the effects of model drift.

In the technique, climatic changes from the GCM experiments are downscaled by interpolation on the

ice-sheet model grid and subsequent superimposition onto the climatic representations employed by the ice-sheet model. For temperature, the following relation was used:

$$\begin{aligned}
 T_{\text{sur}}(\phi, \lambda, t) &= T_{\text{sur}}(\phi, \lambda, \text{present})_{\text{par}} + [T_{\text{sur}}(\phi, \lambda, \text{anomaly}) \\
 &\quad - T_{\text{sur}}(\phi, \lambda, \text{present})]_{\text{time_slice}} \\
 &\quad \times \frac{[\bar{T}_{\text{sur}}^{\text{ice}}(t)_{\text{scenario}} - \bar{T}_{\text{sur}}^{\text{ice}}(t)_{\text{control}}]_{\text{AOGCM_time_series}}}{[\bar{T}_{\text{sur}}^{\text{ice}}(\text{anomaly}) - \bar{T}_{\text{sur}}^{\text{ice}}(\text{present})]_{\text{driving_AOGCM_time_series}}}
 \end{aligned} \tag{1}$$

where T_{sur} is the mean monthly surface temperature referred to the initial ice-sheet topography, $T_{\text{sur}}(\phi, \lambda, \text{present})_{\text{par}}$ is present-day mean monthly surface temperature obtained from parameterisations as a function of latitude and elevation (Huybrechts and de Wolde, 1999), $[T_{\text{sur}}(\phi, \lambda, \text{anomaly}) - T_{\text{sur}}(\phi, \lambda, \text{present})]$ the mean monthly anomaly pattern from either high-resolution AGCM as shown in Figs. 3 and 4, and $\bar{T}_{\text{sur}}^{\text{ice}}$ are mean annual ice-sheet averaged temperature from the respective lower-resolution AOGCM experiments. The driving AOGCMs are either ECHAM4/OPYC3 G or HadCM3 A2 as described above and the forcing time series are those listed in Table 2. Present-day is referred to the year 1975, which is also conveniently situated in the middle of the period 1960–1990 of the climatological reference period. The *anomaly* and *present* periods are those over which the respective GCM averages were considered. We opted to scale the time slices relative to the corresponding ice-sheet averages of the driving AOGCM rather than of the time slices themselves, which are somewhat different, because the former were obtained for similar resolutions as the forcing AOGCMs, and because this approach ensures that the anomaly pattern would be exactly reproduced during the anomaly period were the time slice forced by their own driving AOGCM. The actual surface temperature required for the melt- and runoff model additionally incorporates the effect of changes in surface elevation with the same lapse rate as for the surface temperature parameterisations.

For precipitation, we used ratios rather than differences to avoid the possibility of obtaining

negative precipitation in the event that the AGCM control field deviates significantly from the observed field:

$$\begin{aligned}
 P(\phi, \lambda, t) &= P(\phi, \lambda, \text{present})_{\text{observed}} \\
 &\quad \times \left\{ \left(\frac{[P(\phi, \lambda, \text{anomaly})]}{[P(\phi, \lambda, \text{present})]}_{\text{time_slice}} - 1 \right) \right. \\
 &\quad \times \left. \frac{\left[\frac{\bar{P}_{\text{ice}}(t)_{\text{scenario}}}{\bar{P}_{\text{ice}}(t)_{\text{control}}} - 1 \right]_{\text{AOGCM_timeseries}}}{\left[\frac{\bar{P}_{\text{ice}}(\text{anomaly})}{\bar{P}_{\text{ice}}(\text{present})} - 1 \right]_{\text{driving_AOGCM_time_series}}} + 1 \right\} \\
 &\quad \text{if } \frac{[P(\phi, \lambda, \text{anomaly})]}{[P(\phi, \lambda, \text{present})]}_{\text{time_slice}} > 1
 \end{aligned} \tag{2}$$

where P is precipitation rate and all the subscripts have the same meaning as in Eq. (1). In this case all values of P are considered as mean annual values because reliable information on the monthly distribution of the observed precipitation is not available. Also, the yearly mass balance does not depend very strongly on the monthly distribution of precipitation, which only enters the calculations via the depth of the snow layer in which percolation can take place, and via the rain fraction. The latter depends on surface air temperature and is therefore obtained by assuming an even distribution of precipitation during the year. Summing and subtracting 1 is required to preserve the sign of the fractional increase/decrease with respect to unity.

To avoid negative precipitation, the scaling technique needs to take into account the inverse of the precipitation pattern ratio when this ratio is between 0 and 1 as follows:

$$\begin{aligned}
 P(\phi, \lambda, t) &= P(\phi, \lambda, \text{present})_{\text{observed}} \\
 &\quad \times \left\{ \left(\frac{1}{\left[\frac{P(\phi, \lambda, \text{anomaly})}{P(\phi, \lambda, \text{present})} \right]_{\text{time_slice}}} - 1 \right) \right. \\
 &\quad \times \left. \frac{\left[\frac{\bar{P}_{\text{ice}}(t)_{\text{scenario}}}{\bar{P}_{\text{ice}}(t)_{\text{control}}} - 1 \right]_{\text{AOGCM_timeseries}}}{\left[\frac{\bar{P}_{\text{ice}}(\text{anomaly})}{\bar{P}_{\text{ice}}(\text{present})} - 1 \right]_{\text{driving_AOGCM_time_series}}} + 1 \right\}^{-1} \\
 &\quad \text{if } \frac{[P(\phi, \lambda, \text{anomaly})]}{[P(\phi, \lambda, \text{present})]}_{\text{time_slice}} < 1
 \end{aligned} \tag{3}$$

The pattern scaling technique is subject to several assumptions. The most important is probably that patterns of climate change are necessarily conserved in time. Such a pattern may however arise from various competing processes with different sign, and obviously there is no guarantee that all these processes would scale in time at the same rate. For instance the technique cannot distinguish between precipitation and evaporation/sublimation because a sublimation climatology is not available for the present time. Using total precipitation ratios to force an observed accumulation field which already includes the effects of sublimation thus necessarily assumes that both precipitation and sublimation change by the same fraction, and thus that their relative importance is conserved under conditions of climate change. Fortunately this seems to be roughly the case. Wild et al. (2003) found that total precipitation and sublimation varied by a similar fraction between the two ECHAM4 time slices for both ice sheets, but such behaviour is not given by definition.

The scaling method for temperature also works best when the anomaly pattern is positive, which is also generally the case over both ice sheets. If it were negative, and when the forcing AOGCM time series is also negative, the result would be a positive temperature change that is probably not realistic. Eqs. (1)–(3) fail when the ice-sheet averaged temperature differences or precipitation ratios of the driving AOGCMs are respectively negative or less than unity, but that is not the case for both climate models either.

Table 1 indicates how the ECHAM4 and HadAM3H time slice experiments combine with their underlying driving time series of ECHAM4/OPYC3 G and HadCM3 A2 to provide the mean precipitation sensitivity to temperature changes. For Greenland, the GCM thermodynamic and circulation responses give a range of 5–9%/°C of precipitation increase, somewhat less than indicated by ice-cores for the glacial–interglacial transition (Kapsner et al., 1995; Cuffey and Clow, 1997), but more than for Holocene variability and values used in earlier studies (e.g. Huybrechts and de Wolde, 1999). For Antarctica, on the other hand, the precipitation sensitivity from 21st century time slice simulations of the order 4–7%/°C is more in accord with those inferred from glacial/interglacial contrasts from ice cores (Yiou et al., 1985), which several studies suggested follows a Clausius–Clapeyron argument

(accumulation is proportional to the saturated vapour pressure of the air circulating above the surface inversion layer). The Clausius–Clapeyron average sensitivity was found to be 5.9% for a uniform 1 °C warming (Huybrechts and Oerlemans, 1990). The sensitivity range however additionally varies by scaling with the variety of AOGCMs as temperature and precipitation are treated independently.

4. Results

The results distinguish between the long-term ice-dynamic evolution from past climate changes, extracted from the experiments discussed in Huybrechts (2002), and the effects of modern mass-balance changes as obtained in this study.

4.1. Contributions to global sea-level change

Fig. 6 shows the predicted volume changes expressed in equivalent sea-level changes for the time period between 1860 and 2100 for the two AGCM time slices (panels a and b) forced by the full set of AOGCM time series. The range is quite large, solely reflecting AOGCM inter-model uncertainty in the climate response for the same greenhouse warming scenario. All simulations have in common that Greenland will shrink both during the 20th and 21st century, and thus contribute positively to sea level, and that Antarctica will grow, and thus contribute negatively to sea level. There is also an acceleration in the response for the 21st century. Typically, mass balance changes cause a Greenland contribution of +2 to +7 cm between 1975 and 2100, and an Antarctic contribution of between –2 and –14 cm. Also, both ice sheets combined would contribute negatively to sea level for the 21st century, and this applies to the majority of individual AOGCM time series.

Combining these results with the long-term background trend does not change the picture for Greenland as its background evolution is very small, but gives a less negative sea-level contribution for Antarctica. Here, the background trend of about +2.5 cm per century dominates over the modern mass-balance effect for most of the 20th century, but is of opposite sign. It is only counterbalanced by modern mass-balance changes for the second half of the 21st

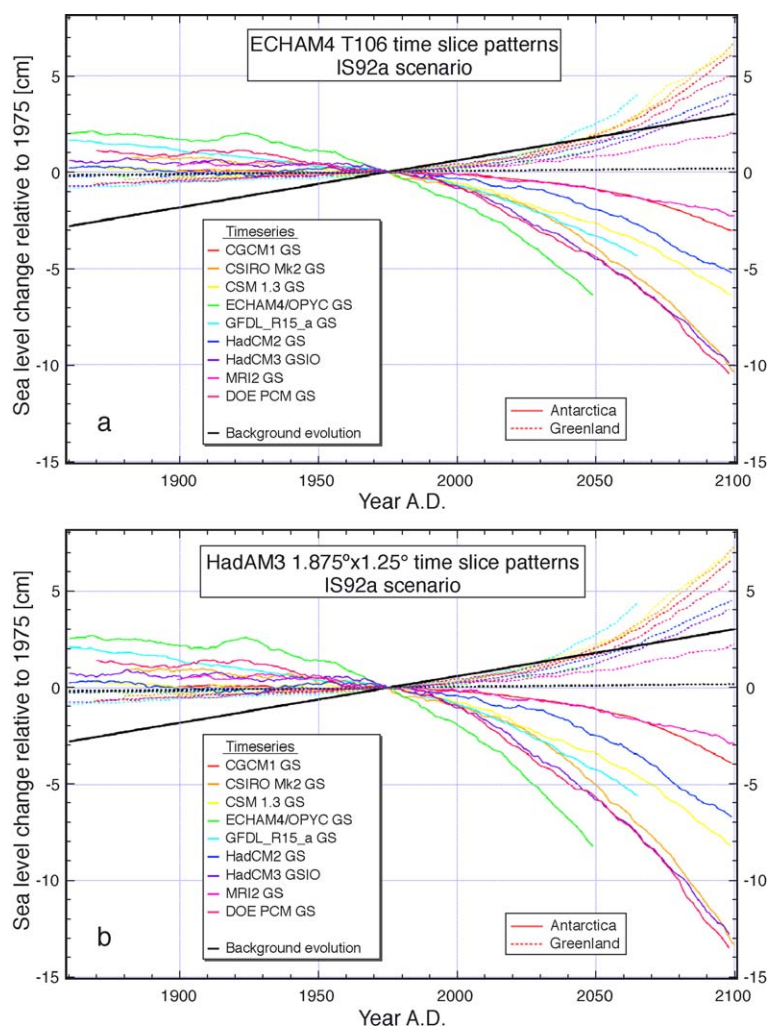


Fig. 6. Volume changes of the Antarctic and Greenland ice sheets expressed in equivalent sea-level change for the various experiments. The results include the ice-dynamic effect from contemporary mass-balance changes but not the background trend resulting from past environmental changes, which is shown separately by the thick black lines. Stippled lines refer to the Greenland ice sheet; the full lines are for the Antarctic ice sheet. The reference time is 1975 A.D. for all experiments. Ice-volume changes were transformed into worldwide sea-level changes by assuming an ice density of 910 kg m^{-3} and a constant oceanic surface area of $3.62 \times 10^8 \text{ km}^2$, or 71% of the Earth's surface.

century. Whereas the different time series produce a wide range of results, the results for the two time slices scaled to the same time series are quite similar, as was already evident from the similarity between ice-sheet averaged values for both AGCMs as given in Table 1.

The mass-balance only results are very similar to those reported for an identical exercise performed for the IPCC TAR (Church et al., 2001) despite a higher model resolution for Antarctica, new precipitation

datasets, and a somewhat more sophisticated melt-and runoff model. As such, they represent a revision to many of the earlier assessments that predicted that both ice sheets would about balance one another. The negative sea-level contribution from the polar ice sheets found here is mainly because of the larger accumulation increases predicted by GCMs and because of the lower summer warming over coastal Greenland, where it counts most for ablation. It is interesting to note that a recent calculation with the

ECHAM4 time slices at the time of CO₂ doubling (~ 2045) yielded a mass gain also for the Greenland ice sheet for the first half of the 21st century (Wild et al., 2003). These authors used another model for ablation, but also a higher local Greenland resolution of 2 km which they found decreased the size of the ablation zone, and therefore of total runoff, a feature already noted in earlier work by Reeh and Starzer (1996) and Van de Wal and Ekholm (1996).

On average, combining the mass-balance components with the background evolution for both ice sheets gives a slightly positive contribution to sea level during the 20th century (+1.8 cm) and a slightly negative contribution during the 21st century (–0.4 cm), but the associated error bars do not enable us to distinguish

this evolution from a zero trend, cf. Table 3 for an overview of the rates involved. These results are for the mid-range IS92a scenario only. Taking into account other scenarios and other sources of uncertainty would make the range of predictions even larger.

4.2. Patterns of ice thickness change

The patterns of 20th century ice thickness change are shown in Figs. 7 and 8. The mass-balance only results (panels b and c) have been taken from the experiments forced by an average time series (HadCM3 GSIO). Again, both time-slice patterns produce quite similar results. For Antarctica, the patterns are characterized by thickening rates of the

Table 3

Century-averaged rates of mass changes of the Antarctic and Greenland ice sheets from all experiments discussed in this paper

	Greenland 20th century [mm/year sea-level equivalent]	Greenland 21st century [mm/year sea-level equivalent]	Antarctica 20th century [mm/year sea-level equivalent]	Antarctica 21st century [mm/year sea-level equivalent]
ECHAM4 T106 patterns				
CGCM1 GS	+0.058	+0.593	–0.024	–0.294
CSIRO Mk2 GS	+0.054	+0.655	–0.158	–0.960
CSM 1.3 GS	+0.067	+0.605	–0.039	–0.584
ECHAM4/OPYC3 GS	+0.039	+0.179	–0.319	–1.001
GFDL_R15_a GS	+0.095	+0.573	–0.167	–0.565
HadCM2 GS	+0.033	+0.394	–0.022	–0.498
HadCM3 GSIO	+0.057	+0.366	–0.093	–0.925
MRI2 GS	+0.015	+0.186	–0.085	–0.213
DOE PCM GS	+0.101	+0.481	–0.186	–0.994
Mean for all IS92a GS timeseries	+0.058 ± 0.028	+0.448 ± 0.178	–0.121 ± 0.096	–0.670 ± 0.308
ECHAM4/OPYC3 G	+0.083	+0.470	–0.223	–0.968
HadAM3H 1.875° × 1.25° patterns				
CGCM1 GS	+0.063	+0.648	–0.028	–0.378
CSIRO Mk2 GS	+0.059	+0.716	–0.199	–1.247
CSM 1.3 GS	+0.082	+0.666	–0.049	–0.748
ECHAM4/OPYC3 GS	+0.043	+0.195	–0.407	–1.287
GFDL_R15_a GS	+0.101	+0.623	–0.212	–0.724
HadCM2 GS	+0.036	+0.435	–0.027	–0.645
HadCM3 GSIO	+0.063	+0.401	–0.120	–1.196
MRI2 GS	+0.018	+0.202	–0.108	–0.272
DOE PCM GS	+0.108	+0.525	–0.225	–1.284
Mean for all IS92a GS timeseries	+0.063 ± 0.030	+0.490 ± 0.195	–0.153 ± 0.123	–0.865 ± 0.400
HadCM3 A2	+0.049	+0.419	–0.201	–1.312
Long-term background trend				
Runs of this paper	+0.015		+0.243	

The rates quoted for ECHAM4/OPYC3 G and HadCM3 A2 are for the respective time-slice experiments forced by their own driving AOGCM. These follow a somewhat different climate scenario, and are therefore not taken into account to calculate average trends. The error on the mean is for 1 standard deviation. All values are expressed in mm/year of equivalent global sea-level change.

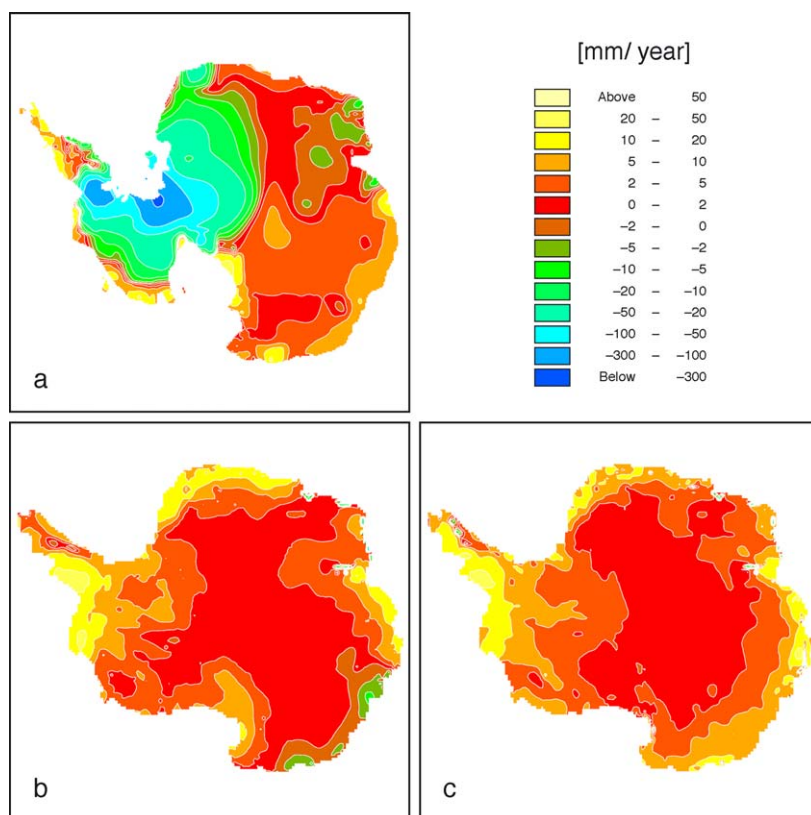


Fig. 7. Patterns of average ice thickness change during the 20th century for Antarctica for the experiments forced by the HadCM3 GSIO time series. (a) Long-term background trend from a model run over the last 4 glacial cycles. (b) Thickness changes obtained with the ECHAM4 time slices. (c) Thickness changes obtained with the HadAM3H time slices. The long-term trend is shown for grounded ice only. The 20th century thickness changes include surface accumulation changes on the ice shelves. Values are expressed in mm/year of local ice thickness change.

order of several mm to a few cm per year modulated in accordance with the anomaly fields. Melting is generally absent, except locally along the lower reaches of the Lambert Glacier (Amery Ice Shelf), coastal Enderby and Wilkes Land and along the eastern flank of the Antarctic Peninsula. The thickening pattern is qualitatively similar to the long-term background evolution over much of East Antarctica (panel a), but is more than counteracted by quite large thinning rates up to 30 cm/year over the West Antarctic ice sheet, related to ongoing grounding line retreat since the LGM. This thinning is most pronounced along the Weddell Sea margin, where most recent retreat is found to have taken place, and fans out to nearby parts of the East Antarctic ice sheet. The ongoing thickening of several mm/year in interior areas of East Antarctica is a direct consequence of

the roughly doubling of accumulation rates following the last glacial–interglacial transition between 15 and 10 kyears BP.

For Greenland, the long-term background pattern (Fig. 8, panel a) shows a small thickening over the accumulation area, more pronounced over the southern half, and a larger thinning over the ablation area, however with little overall effect on sea level. The single most important explanation for this pattern is the recovery of the ice sheet from the Little Ice Age cooling which ended about 200 years ago, leading to both higher accumulation and run-off rates. Superimposed on this pattern are the effects of basal warming following the last glacial–interglacial transition, the downward propagation of the harder Holocene ice, and heat conduction in the bedrock, as discussed in more detail in Huybrechts (1994) and

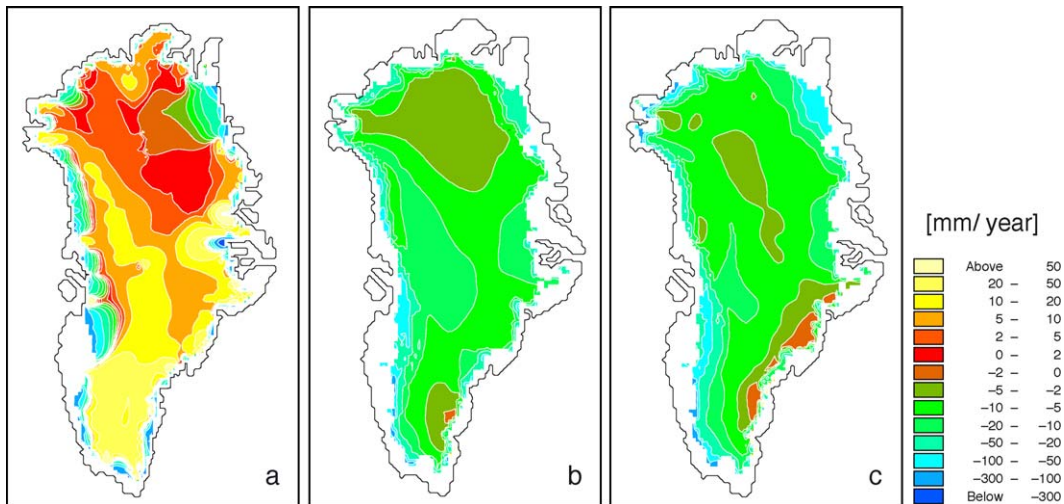


Fig. 8. Patterns of average ice thickness change during the 20th century for Greenland for the experiments forced by the HadCM3 GSIO time series. (a) Long-term background trend from a model run over the last two glacial cycles. (b) Thickness changes obtained with the ECHAM4 time slices. (c) Thickness changes obtained with the HadAM3H time slices. Values are expressed in mm/year of local ice thickness change.

Huybrechts and Le Meur (1999). The 20th century pattern of mass changes (Fig. 8, panels b and c) is at odds with the long-term trend and displays slight thinning all over the Greenland ice sheet. That is because precipitation is on average predicted to decrease over the 20th century. This occurs together with a small 20th century warming leading to some increased ablation at the margin.

Evolution patterns for the 21st century are much more clear signatures of a climatic warming (Figs. 9 and 10). This leads to a thickening over most of East

and West Antarctica of up to several tens of cm/year in the Amundsen Sea sector, where current precipitation rates are highest. Thinning is only found in some coastal areas where it is either due to a precipitation ratio less than unity (Wilkes Land in ECHAM4), or some runoff in areas characterized by low precipitation rates (Siple Coast, Lambert Glacier). Note that the results over the ice shelves show only the effects of accumulation changes. Basal melting below the ice shelves is not considered, and it is furthermore assumed that any surface melting does not run off

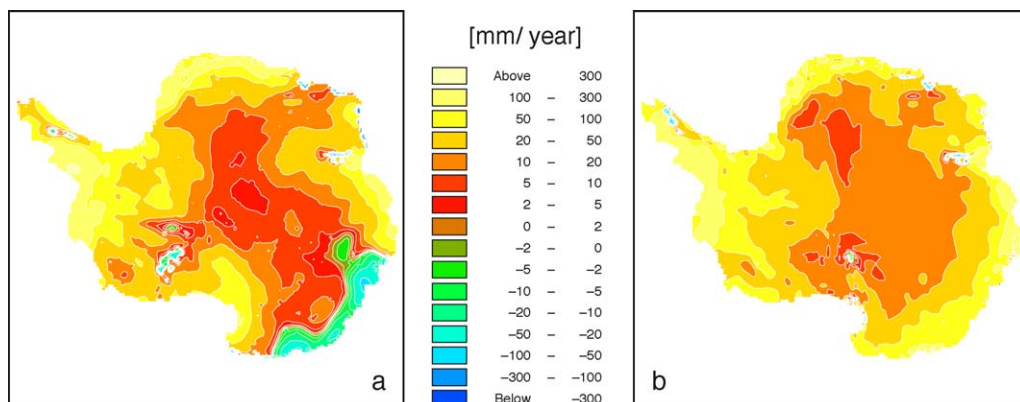


Fig. 9. Patterns of average ice thickness change during the 21st century for Antarctica for the experiments forced by the HadCM3 GSIO time series. (a) Thickness changes obtained with the ECHAM4 time slices. (b) Thickness changes obtained with the HadAM3H time slices. The results include surface accumulation changes on the ice shelves.

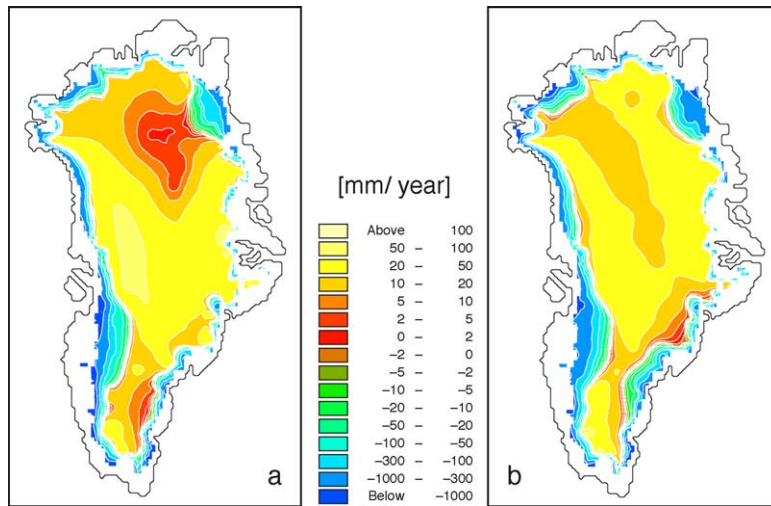


Fig. 10. Patterns of average ice thickness change during the 21st century for Greenland for the experiments forced by the HadCM3 GSIO time series. (a) Thickness changes obtained with the ECHAM4 time slices. (b) Thickness changes obtained with the HadAM3H time slices.

because of the very small surface slopes, but refreezes in situ during the winter season. Over Greenland, there is a clear thickening above the equilibrium line of several cm/year and a thinning by several m/year in the ablation area as expected from the rising temperature and precipitation trends.

4.3. Sensitivity of the results to the model setup

Sensitivity experiments were performed to test the way climatic changes are imposed, distinguish how

temperature and precipitation influence the mass balance, and investigate the role of ice dynamics on the ice sheet’s response. These are demonstrated for the HadAM3H patterns in combination with the HadCM3 GSIO time series. This combination gives a total response at the higher end of the range of simulations for Antarctica, but close to average for Greenland.

The results for the Antarctic ice sheet are shown in Fig. 11. It can be seen that it does not make much difference whether precipitation differences rather than

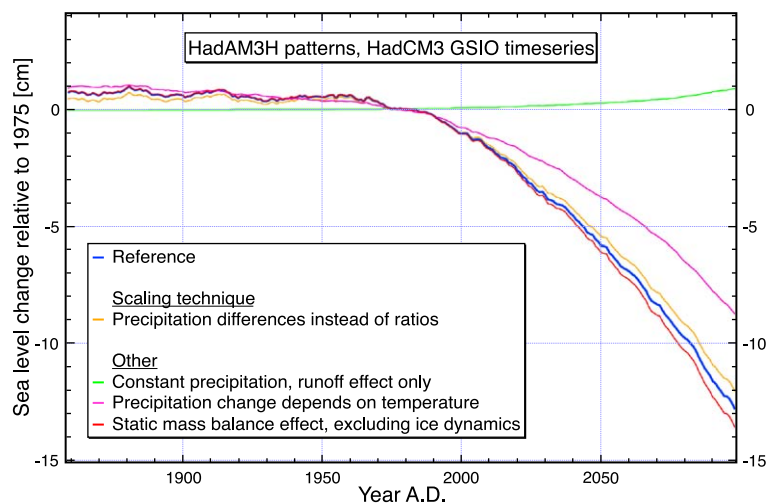


Fig. 11. Sensitivity of the Antarctic results to changes in the pattern scaling technique and other details of the model setup as indicated.

precipitation ratios are imposed. This variant was implemented by a modification of Eq. (1) in which T was replaced by P . The reason for the similar response is that on average the precipitation distribution from the AGCM time slice is very close to the observed precipitation distribution, in which case both methods can be interchanged. The precipitation increase in this experiment is also a bit larger than that derived from the saturation vapour pressure argument used in older work (e.g. Huybrechts and de Wolde, 1999) to link precipitation changes to temperature changes. This larger sensitivity suggests that in a warmer climate changes in atmospheric circulation and increased moisture advection (less sea ice, warmer ocean surface) can also become important to enhance precipitation, in particular close to the ice-sheet margin, but the result obtained here is also in part because of the HadAM3H/HadCM3 GSIO combination, which already has a higher than average precipitation increase. For Antarctica, excluding the ice-dynamic response to the imposed mass-balance changes hardly affects the result because of the small ice-dynamic response (<5%) discussed for the century time scale in previous work (Huybrechts and de Wolde, 1999). The contribution from runoff is also small at less than +1 cm of sea level rise, or about 7% of the precipitation response, as evident from the constant precipitation experiment.

For Greenland, the response is most sensitive to the seasonality of the temperature anomaly (Fig. 12). Considering yearly temperature patterns rather than monthly temperature patterns doubles the response because the summer warming was found to be much less than the annual average. The sensitivity results also demonstrate that even on a century time scale, Greenland ice-sheet dynamics cannot be neglected and counteracts the mass-balance only response (static effect) by up to 10–20% by the end of the 21st century. For Greenland, the temperature effect appears clearly dominant: the effect of precipitation changes only (at constant temperature) makes the ice sheet grow equivalent to about 1 cm of sea-level lowering by the end of the 21st century when forced with HadCM3 GSIO time series, or about 20% of the total response. This does not confirm the results obtained with the ECHAM4 timeslices in Van de Wal et al. (2001) and Wild et al. (2003), who found the effect of precipitation changes for Greenland much more important to counteract the increased runoff associated with 21st century warming. A comparison with the experiment in which changes of the precipitation rate are directly linked to the temperature change (at 5% per °C as in previous work) nicely demonstrates how the 20th century volume decrease is almost entirely caused by a precipitation decrease rather than a temperature and runoff increase. It also suggests a larger precipitation sensitivity during the

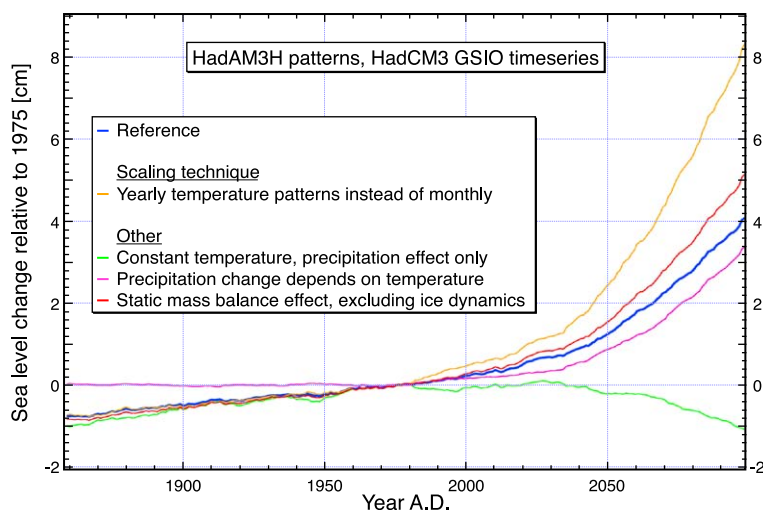


Fig. 12. Sensitivity of the Greenland results to changes in the pattern scaling technique and other details of the model setup as indicated.

21st century than suggested from late Holocene ice-core records, from which the 5% value was inferred (Clausen et al., 1988).

4.4. Comparison with observations

A comparison of the simulations with observations can only be made for the 20th century, but is hampered by the scarcity of data in both space and time. Nevertheless, available measurements allow us to assess qualitative aspects of the results obtained in this paper. A distinction should be made between meteorological or climate data on temperature and precipitation changes, to be compared to the climate forcing, and observations on surface elevation changes, to be compared to the final results.

Direct meteorological series are however few, and are almost exclusively limited to coastal stations. Longer series only exist for Greenland, but are often not homogenous. For Antarctica, such records only extend back to the International Geophysical Year of 1957–1958. Additional insight is available from meteorological re-analyses (ECMWF, NCEP-NCAR) and AGCM simulations driven by observed SSTs, but only for the second half of the 20th century. Accumulation estimates from shallow ice cores, on the other hand, cover longer time periods but are limited to a few sites only.

The general picture that can be distilled from these data is in reasonable agreement with many aspects derived from the GCMs in this paper forced by historical greenhouse gas concentrations. Various sources indicate that Greenland is a regional exception to the warming trend observed in many other places on Earth for much of the second half of the 20th century. Hanna and Cappelen (2003) found a significant cooling trend between 1958 and 2001 in coastal southern Greenland of -1.3 °C in contrast to a global warming trend over the same period. Bromwich et al. (1993) found a decreasing trend in precipitation of about 15% between 1963 and 1988. Results from long-term (1950–1991) climate simulations with the T63 resolution CSIRO9 AGCM forced by observed SST also indicate that net accumulation decreased in analogy with a decreasing surface temperature over the ice sheet and a cooling over the surrounding ocean (Smith, 1999). The cooling over the 41-year period was found to be 0.66 °C with

a precipitation decrease of 13% over the ice sheet consistent with the results from Bromwich et al. (1993). Bales et al. (2001) report a decreasing trend in accumulation in a location in northwest Greenland for the second half of the 20th century of 25%. Although these observations do not span the whole 20th century, they certainly do not contradict the most conspicuous feature of the climate forcing found in this study, namely the decreasing precipitation trend on average, which resulted in a thinning over the accumulation zone from 20th century mass balance changes alone. The small overall warming trend predicted by most of the AOGCMs over Greenland for the whole of the 20th century, on the other hand, is also supported by the few long temperature records available from coastal sites (Box, 2002).

Available data from Antarctica are all indicative of a mean warming trend concomitant with an increase of precipitation during the 20th century, but with highly variable regional responses. Turner et al. (2002) derived a spatially weighted warming trend of 0.176 °C per decade between 1958 and 2002 over all of Antarctica, less than the $+1.2$ °C for all Antarctic stations between 1959 and 1996 (Vaughan et al., 2001). Since most of these stations are at the coast, this is consistent with a weak cooling over the interior of the Antarctic continent (Thompson and Solomon, 2002). The most significant warming occurred over the Antarctic Peninsula, especially at its western side where the trend is $+0.56$ °C per decade for 1951–2001 or a total of $+2.8$ °C. This local trend is completely missing from the GCM derived forcing used here, a feature already discussed for comparable GCM results obtained for the second half of the 20th century elsewhere (Connolley and O'Farrell, 1998; Vaughan et al., 2001). Our 20th century precipitation forcing however agrees better with the increasing trend of 5% over all of Antarctica established from moisture budget analysis between 1955 and 1975 (Bromwich and Robasky, 1993). Such a positive trend is confirmed by an increase in snow accumulation at South Pole station since 1965 of possibly up to 30% as derived from ice cores (Mosley-Thompson et al., 1999). Significant increases of snow accumulation of up to 20% since the 1960s were also derived from four ice cores in Wilkes Land (Morgan et al., 1991), together with a smaller, but still significant increase for all of the 20th century. Simulations with CSIRO9

T63 forced with observed SSTs over the period 1950–1991 (Smith et al., 1998) gave an average Antarctic warming of $+0.74$ °C, or $+0.18$ °C per decade, with a concomitant increase of accumulation of 4.1%, or 1% per decade. The average precipitation trend from all our simulations with the two time-slice patterns scaled by all AOGCMs was 2.7% for the whole 20th century, lower than some of the numbers cited above but representative for a longer period (Table 3).

The combined present-day evolution patterns (long-term and 20th century) of Antarctic and Greenland ice thickness change (Figs. 7 and 8) also seem to share many of the features derived from recent observational data, in particular from repeated airborne laser altimeter and satellite radar altimeter measurements over the last decade (Rignot and Thomas, 2002). These indicate a slight mass loss for the Greenland ice sheet equal to about $+0.1$ mm/year of sea level change, together with a clear mass loss for West Antarctica and no clear trend yet for East Antarctica. The spatial pattern for Greenland agrees rather well with these direct measurements for the nineties, showing a slight thickening or an approximate balance for the accumulation zone together with a general pattern of thinning for the ablation zone. The only deviation to this general picture is the stronger thinning exceeding 1 m/year close to the coast in southeast Greenland (Krabill et al., 2000). This feature is therefore likely to be of ice-dynamic origin for a mechanism not incorporated in the modeling (the category of ‘unexpected ice-dynamic responses’ as discussed in the introduction). The same remark applies to the inferred late 20th century pattern of changes of the West Antarctic ice sheet, where available data seem to point to a thickening in the north (Siple Coast ice streams) and a thinning in the west (in particular for the Amundsen Sea sector). That is different from what the modeling produces, probably for similar reasons as for southeast Greenland.

The small thickening over large parts of the East Antarctic plateau, on the other hand, both from the long-term response as from 20th century mass-balance changes, seems to agree better with ERS1/2 data obtained between 1992 and 1996 (Wingham et al., 1998). It should however be noted that the modeling results refer to a century trend, whereas the observational data are only for one or two decades at most, and therefore of too short a duration to confidently

distinguish between short-term variability and the longer-term trend. In addition, the altimetry data are for surface elevation. They are therefore contaminated by an unknown component from crustal uplift when compared with ice thickness changes, though modeling studies indicate that bedrock changes are usually an order of magnitude smaller than ice thickness changes on a century time scale (Huybrechts and Le Meur, 1999).

5. Summary and conclusion

Pattern scaling appears to be a useful technique to predict climatic changes over the ice sheets. Although the technique should be used with care, and full interactive coupling with transient AOGCMs at high resolution would be preferable, the strength of the method is its flexibility to generalise to other climate scenarios while at the same time incorporating temporal and spatial patterns of climate change in the best possible way from current GCM simulations.

A very robust feature of all experiments for the 21st century is that the Antarctic ice sheet is predicted to grow and the Greenland ice sheet is predicted to shrink because of the dominance of increased precipitation and increased runoff, respectively. These trends are significantly different from zero within 2 sigma error bars (Table 3). Trends from mass-balance changes alone are also significant for the 20th century but the process for the Greenland ice sheet is found to be different, with decreased precipitation rather than increased runoff as the major source of the mass loss. For the majority of driving AOGCMs, the Antarctic response is larger than for Greenland, so that the combined sea-level contribution from polar ice sheets during the 21st century from mass-balance changes alone is negative. This conclusion no longer holds when including the background trends found in this study, that are in the middle of the IPCC TAR range obtained from all methods, in which case both ice sheets combined would yield an evolution that is indistinguishable from a zero trend. Ice-dynamic effects to the imposed 20th and 21st century mass changes are of second-order importance.

The experiments discussed here considered only one emission scenario and one set of ice-sheet model

and mass-balance model parameters and therefore highlight the uncertainty introduced by the variability in the climate models. It is certainly comforting that most of the variability comes from the spread of inherent climate sensitivity of the underlying AOGCM simulations. There is a great similarity in both qualitative aspects of the patterns as in average changes over time for both time-slice patterns forced by the same AOGCM time series. More AGCM patterns should however be used in future work to confirm whether this is a robust result or whether this outcome was overly conditioned by the choice of model and the specific pattern scaling method employed.

The experiments with the ECHAM4 time slice patterns (Wild and Ohmura, 2000) were used as the base for the IPCC TAR projections of sea-level rise from the polar ice sheets (Church et al., 2001), albeit with some slight changes in the ice-sheet and mass-balance models. To do that, these results were regressed against global mean temperature to enable further scaling to take into account the complete range of IPCC temperature predictions for the most recent SRES scenarios. Taking into account the background evolution and various other sources of uncertainty, this yielded a predicted Antarctic contribution to global sea-level change between 1990 and 2100 of between -19 and $+5$ cm, which range can be considered as a 95% confidence interval. For Greenland, the range was -2 to $+9$ cm. Most of this spread came from the climate sensitivity of the forcing AOGCMs, and less from the emission scenario or the uncertainty in the ice-sheet models.

For the runs in this paper we find a total range of polar ice-sheet response of between $+5$ and -12 cm during the period 1990–2100 for any combination of both ice sheet results together. Including the long-term background trend the range is between $+8$ and -9 cm, not significantly different from zero but with a slightly higher mean than in the IPCC TAR. This leaves thermal expansion of the seawater and melting of mountain glaciers and small ice caps as major sources of sea level rise during the 21st century. In the IPCC TAR, using the same set of AOGCMs as used in this paper, the corresponding sea-level contributions from the latter sources were found to be in the ranges $+0.11$ – 0.43 m and $+0.01$ – 0.23 cm, respectively. For sustained greenhouse warming con-

ditions beyond the 21st century, however, the approximate balance between the two polar ice sheets may no longer hold and both ice masses may significantly start to melt at rates of up to 10 mm/year of sea level rise (Huybrechts and de Wolde, 1999).

Acknowledgements

This work was performed within the scope of the German HGF-Strategiefonds Projekt 2000/13 SEAL (Sea Level Change), and the Belgian Global Change and Sustainable Development Programme (Federal Office for Scientific, Technical, and Cultural Affairs, Prime Minister's Service) under contracts CG/DD/09B and EV/03/9B. We are grateful to David Hassell, Richard Jones and James Murphy for HadAM3H data. Work at the Hadley Centre was supported by the UK Department for Environment, Food and Rural Affairs under contract PECD 7/12/37 and by the Government Meteorological Research and Development Programme. The high resolution ECHAM experiments became possible through the generous computing resources provided by the Swiss Center for Scientific Computing CSCS, and through the support of the National Center for Competence in Climate Research (NCCR Climate).

References

- Bales, R.C., Mosley-Thompson, E., McConnell, J.R., 2001. Variability of accumulation in northwest Greenland over the last 250 years. *Geophysical Research Letters* 28 (14), 2679–2682.
- Bindschadler, R.A., Bentley, C.R., 2002. On thin ice? *Scientific American* (12), 66–73.
- Box, J.E., 2002. Survey of Greenland instrumental temperature records: 1873–2001. *International Journal of Climatology* 22, 1829–1847.
- Bromwich, D.H., Robasky, F.M., 1993. Recent precipitation trends over the polar ice sheets. *Meteorology and Atmospheric Physics* 51, 259–274.
- Bromwich, D.H., Robasky, F.M., Keen, R.A., Bolzan, J.F., 1993. Modeled variations of precipitation over the Greenland ice sheet. *Journal of Climate* 6, 1253–1268.
- Bromwich, D.H., Cullather, R.I., van Woert, M.L., 1998. Antarctic precipitation and its contribution to the global sea-level budget. *Annals of Glaciology* 27, 220–226.
- Church, J.A., Gregory, J.M., Huybrechts, P., Kuhn, M., Lambeck, K., Nhuon, M.T., Qin, D., Woodworth, P.L., 2001. Changes in sea level. In: Houghton, J.T., Ding, Y., Griggs, D.J., Noguero,

- M., Van der Linden, P.J., Dai, X., Maskell, K., Johnson, C.A. (Eds.), *Climate Change 2001: The Scientific Basis: Contribution of Working Group I to the Third Assessment Report of the Intergovernmental Panel on Climate Change*. Cambridge Univ. Press, Cambridge, pp. 639–694.
- Clausen, H.B., Gundestrup, N.S., Johnsen, S.J., Bindshadler, R.A., Zwally, H.J., 1988. Glaciological investigations in the crete area, central Greenland. A search for a new drilling site. *Annals of Glaciology* 10, 10–15.
- Connolley, W.M., O'Farrell, S.P., 1998. Comparison of warming trends over the last century around Antarctica from three coupled models. *Annals of Glaciology* 27, 565–570.
- Cubasch, U., Waszkewitz, J., Hegerl, G.C., Perlwitz, J., 1995. Regional climate changes as simulated in time-slice experiments. *Climatic Change* 31, 273–304.
- Cuffey, K.M., Clow, G.D., 1997. Temperature, accumulation, and ice sheet elevation in central Greenland through the last deglacial transition. *Journal of Geophysical Research* 102 (C12), 26383–26396.
- De Wolde, J., Huybrechts, P., Oerlemans, J., van de Wal, R.S.W., 1997. Projections of global mean sea level rise calculated with a 2D energy-balance climate model and dynamic ice sheet models. *Tellus* 49A (4), 486–502.
- Fichefet, T., Poncin, C., Goosse, H., Huybrechts, P., Janssens, I., Le Treut, H., 2003. Implications of changes in freshwater flux from the Greenland ice sheet for the climate of the 21st century. *Geophysical Research Letters* 30 (17), 1911 (doi:10.1029/2003GL017826).
- Gordon, C., Cooper, C., Senior, C.A., Banks, H., Gregory, J.M., Johns, T.C., Mitchell, J.F.B., Wood, R.A., 2000. The simulation of SST, sea ice extents and ocean heat transports in a version of the Hadley Centre coupled model without flux adjustments. *Climate Dynamics* 16, 147–168.
- Hanna, E., Cappelen, J., 2003. Recent cooling in coastal southern Greenland and relation with the North Atlantic Oscillation. *Geophysical Research Letters* 30 (3), 1132 (doi:10.1029/2002GL015797).
- Hanna, E., Valdes, P., 2001. Validation of ECMWF (re)analysis surface climate data, 1979–98, for Greenland and implications for mass balance modelling of the ice sheet. *International Journal of Climatology* 21, 171–195.
- Houghton, J.T., Ding, Y., Griggs, D.J., Noguera, M., Van der Linden, P.J., Dai, X., Maskell, K., Johnson, C.A. (Eds.), 2001. *Climate Change 2001: The Scientific Basis: Contribution of Working Group I to the Third Assessment Report of the Intergovernmental Panel on Climate Change*. Cambridge Univ. Press, Cambridge, 881 pp.
- Huybrechts, P., 1994. The present evolution of the Greenland ice sheet: an assessment by modelling. *Global and Planetary Change* 9 (1–2), 39–51.
- Huybrechts, P., 2002. Sea-level changes at the LGM from ice-dynamic reconstructions of the Greenland and Antarctic ice sheets during the glacial cycles. *Quaternary Science Reviews* 21 (1–3), 203–231.
- Huybrechts, P., de Wolde, J., 1999. The dynamic response of the Greenland and Antarctic ice sheets to multiple-century climatic warming. *Journal of Climate* 12 (8), 2169–2188.
- Huybrechts, P., Le Meur, E., 1999. Predicted present-day evolution patterns of ice thickness and bedrock elevation over Greenland and Antarctica. *Polar Research* 18 (2), 299–308.
- Huybrechts, P., Oerlemans, J., 1990. Response of the Antarctic Ice Sheet to future greenhouse warming. *Climate Dynamics* 5, 93–102.
- Huybrechts, P., Letréguilly, A., Reeh, N., 1991. The Greenland ice sheet and greenhouse warming. *Global and Planetary Change Section 3* (4), 399–412.
- Huybrechts, P., Steinhage, D., Wilhelms, F., Bamber, J.L., 2000. Balance velocities and measured properties of the Antarctic ice sheet from a new compilation of gridded datasets for modeling. *Annals of Glaciology* 30, 52–60.
- Huybrechts, P., Janssens, I., Poncin, C., Fichefet, T., 2002. The response of the Greenland ice sheet to climate changes in the 21st century by interactive coupling of an AOGCM with a thermo-mechanical ice-sheet model. *Annals of Glaciology* 35, 409–415.
- Janssens, I., Huybrechts, P., 2000. The treatment of meltwater retention in mass-balance parameterizations of the Greenland ice sheet. *Annals of Glaciology* 31, 133–140.
- Joughin, I., Tulaczyk, S., Bindshadler, R.A., Price, S., 2002. Changes in west Antarctic ice stream velocities: observation and analysis. *Journal of Geophysical Research* 107 (B11), 2289 (doi:10.1029/2001JB001029).
- Jung-Rothenhäusler, F., 1998. Remote sensing and GIS studies in North-East Greenland. *Berichte zur Polarforschung* 280, 161 pp.
- Kapsner, W.R., Alley, R.B., Shuman, C.A., Anandakrishnan, S., Grootes, P.M., 1995. Dominant influence of atmospheric circulation on snow accumulation in Greenland over the past 18,000 years. *Nature* 373, 52–54.
- Krabill, W.B., Abdalati, W., Frederick, E., Manizade, S., Martin, C., Sonntag, J., Swift, R., Thomas, R.H., Wright, W., Yungel, J., 2000. Greenland ice sheet: high-elevation balance and peripheral thinning. *Science* 289, 428–430.
- Leggett, J., Pepper, W.J., Swart, R.J., 1992. Emissions scenarios for IPCC: an update. In: Houghton, J.T., Callander, B.A., Varney, S.K. (Eds.), *Climate Change 1992, The Supplementary Report to the IPCC Scientific Assessment*. Cambridge Univ. Press, Cambridge, pp. 69–96.
- Morgan, V.I., Goodwin, I.D., Etheridge, D.M., Wookey, C.W., 1991. Evidence from Antarctic ice cores for recent increases in snow accumulation. *Nature* 354, 58–60.
- Mosley-Thompson, E., Paskievitch, J.F., Gow, A.J., Thompson, L.G., 1999. Late 20th century increase in South Pole accumulation. *Journal of Geophysical Research* 104 (D4), 3877–3886.
- Nakicenovic, N., et al., 2000. *IPCC Special Report on Emissions Scenarios*. Cambridge Univ. Press, Cambridge, 599 pp.
- O'Farrell, S.P., McGregor, J.L., Rotstain, L.D., Budd, W.F., Zweck, C., Warner, R.C., 1997. Impact of transient increases in atmospheric CO₂ on the accumulation and mass balance of the Antarctic ice sheet. *Annals of Glaciology* 25, 137–144.
- Ohmura, A., 2001. Physical basis for the temperature-based melt-index method. *Journal of Applied Meteorology* 40 (4), 753–761.
- Ohmura, A., Reeh, N., 1991. New precipitation and accumulation maps for Greenland. *Journal of Glaciology* 37, 140–148.

- Pope, V.D., Gallani, M.L., Rowntree, P.R., Stratton, R.A., 2000. The impact of new physical parametrizations in the Hadley Centre climate model—HadAM3. *Climate Dynamics* 16, 123–146.
- Reeh, N., Starzer, W., 1996. Spatial resolution of ice-sheet topography: influence on Greenland mass-balance modelling. *Rapport-Grønlands Geologiske Undersøgelse* (53), 85–94.
- Rignot, E.J., Thomas, R.H., 2002. Mass balance of polar ice sheets. *Science* 297, 1502–1506.
- Roeckner, E., et al., 1996. The atmospheric general circulation model ECHAM-4: model description and simulation of present-day climate. Max-Planck-Institut für Meteorologie, Hamburg, Report 218, 90 pp.
- Roeckner, E., Bengtsson, L., Feichter, J., Lelieveld, J., Rohde, H., 1999. Transient climate change simulations with a coupled atmosphere–ocean GCM including the tropospheric sulfur cycle. *Journal of Climate*, 3004–3032.
- Shepherd, A., Wingham, D.J., Mansley, J.A.D., 2002. Inland thinning of the Amundsen Sea sector, West Antarctica. *Geophysical Research Letters* 29 (10) (doi:10.1029/2001GL014183).
- Smith, I.N., 1999. Estimating mass balance components of the Greenland ice sheet from a long-term GCM simulation. *Global and Planetary Change* 20, 19–32.
- Smith, I.N., Budd, W.F., Reid, P., 1998. Model estimates of Antarctic accumulation rates and their relationship to temperature changes. *Annals of Glaciology* 27, 246–250.
- Thompson, D.W.J., Solomon, S., 2002. Interpretation of recent southern hemisphere climate change. *Science* 296, 895–899.
- Turner, J., King, J.C., Lachlan-Cope, T.A., Jones, P.D., 2002. Recent temperature trends in the Antarctic. *Nature* 418, 291–292.
- Van de Wal, R.S.W., Ekholm, S., 1996. On elevation models as input for mass balance calculations of the Greenland ice sheet. *Annals of Glaciology* 23, 181–186.
- Van de Wal, R.S.W., Oerlemans, J., 1997. Modelling the short term response of the Greenland ice sheet to global warming. *Climate Dynamics* 13, 733–744.
- Van de Wal, R.S.W., Wild, M., de Wolde, J., 2001. Short-term volume changes of the Greenland ice sheet in response to doubled CO₂ conditions. *Tellus* 53B, 94–102.
- Van der Veen, C.J., 2002. Polar ice sheets and global sea level: how well can we predict the future? *Global and Planetary Change* 32, 165–194.
- Vaughan, D.G., Spouge, J., 2002. Risk estimation of collapse of the West Antarctic ice sheet. *Climatic Change* 52, 65–91.
- Vaughan, D.G., Marshall, G.J., Connolley, W.M., King, J.C., Mulvaney, R., 2001. Devil in the detail. *Science* 293, 1777–1779.
- Warner, R.C., Budd, W.F., 1998. Modelling the long-term response of the Antarctic ice sheet to global warming. *Annals of Glaciology* 27, 161–168.
- Wild, M., Ohmura, A., 2000. Changes in mass balance of the polar ice sheets and sea level under greenhouse warming as projected in high resolution GCM simulations. *Annals of Glaciology* 30, 197–203.
- Wild, M., Calanca, P., Scherrer, S.C., Ohmura, A., 2003. Effects of polar ice sheets on global sea level in high-resolution greenhouse scenarios. *Journal of Geophysical Research* 108 (D5), 4165 (doi:10.1029/2002JD002451).
- Wingham, D.J., Ridout, A.J., Scharroo, R., Arthern, R.J., Shum, C.K., 1998. Antarctic elevation change from 1992 to 1996. *Science* 282, 456–458.
- Yiou, F., Raisbeck, G.M., Bourles, D., Lorius, C., Barkov, N.I., 1985. ¹⁰Be in ice at Vostok Antarctica during the last climatic cycle. *Nature* 316, 616–617.